Modeling of Atomization Under Flash Boiling Conditions

Yangbing Zeng and Chia-Fon Lee
Department of Mechanical Engineering
University of Illinois at Urbana-Champaign
Urbana, IL, USA

ABSTRACT

This paper presents an atomization model for sprays under flash boiling conditions. The atomization is represented by the secondary breakup of a bubble/droplet system, and the breakup is considered as the results of two competing mechanisms, aerodynamic force and bubble growth. The model was applied to predict the atomization of a hollow-cone spray from pintle injector under flash boiling conditions. In the regimes this study considered, sprays are atomized by bubble growth, which produces smaller SMD's than aerodynamic forces alone. With decreasing ambient pressures, the spray thickness, fuel vaporization rate and vapor radial penetration increases, and the drop size decreases. With increasing the fuel and ambient temperatures to some extent, the effect of flash boiling and air entrainment completely change the spray pattern.

Keywords : flash boiling, atomization, bubble growth, hollow- cone spray

INTRODUCTION

Flash boiling offers great opportunity to improve engine performance due to the improved spray quality compared to conventional jets, such as finer drop sizes, larger spray angles and smaller tip penetration [1]. However, only limited numerical efforts have been made to study the bubble growth and the subsequent breakup process for flash boiling. Lienhard and Day [2] developed a criterion for breakup of superheat jets where the breakup time is taken as the sum of the idle time and the time for the bubble grows up to as large as the initial jet diameter. Oza and Sinnamon [3] assumed that the jet breaks up when the bubble radius grows twice as large as its initial radius. Senda et al. [4] and Adachi et al. [5] used void fraction to determine when the jet breaks up. Razzaghi [6] postulated that the jet is still first atomized through aerodynamical force. However, the produced secondary droplets undergo microexplosion. As our knowledge goes, the models for the atomization under flash boiling conditions are underdeveloped, and arbitrary assumptions are involved for most models.

This paper presents a model for the atomization under flash boiling conditions with intermediate superheat degrees. Under this condition, the effect of vaporization at the jet surface on jet atomization is negligible, and

the spray atomization is represented by the secondary breakup of blobs using a blob model. The model details are presented next.

MATHEMATICAL MODEL

Blob Model

Following the original blob model proposed by Reitz and Diwakar [7], the atomization is modeled as the secondary breakup of the blobs, which is due to flash boiling and aerodynamical force in this study. The characteristic size of blobs is determined by

$$r_c = \left(\frac{1}{N_0}\frac{3}{4\pi}\right)^{1/3} \tag{1}$$

where N_0 is the number density of bubbles. N_0 can be related to the superheat of the spray,

$$N_0 = C\exp\left(\frac{A}{\Delta T}\right) \tag{2}$$

where C and A are constants depending on fuels, and ΔT is the superheat degree of the spray defined as the difference between liquid temperature and the saturate temperature at ambient pressure. Equation (1) implies that there is only one bubble in a blob.

As shown in Fig. 1, three regions are present for the bubble/droplet system defined above and each region satisfies its own mass and momentum conservation equations. For Region III, P is assumed to be uniform and is determined by the phase equilibrium. The bubble growth rate can be given by the Rayleigh equation [8].

It is well known that the relative motion at interface is primarily responsible for the system breakup. For the bubble-droplet system defined in this study, two relative motions exist, (1) translational motion between the droplet and ambient gas, and (2) the radial expansion of the droplet and the internal bubble. In this study, translational motion and radial expansion are considered separately. For convenience, the breakup due to the first relative motion is usually referred as aerodynamic breakup. A modified TAB model was developed for the aerodynamic breakup. For the breakup caused by bubble expansion, the breakup criterion is given by a linear stability analysis, and the properties of secondary droplets are given by conservation laws. The coupling effect between these two motions is ignored, and the later results show that the aerodynamic breakup may not be important for a wide range of superheat degrees considered in this paper. The model details are presented in the next two sections.

Aerodynamic Breakup

The TAB model [9] was modified to predict the aerodynamic breakup by incorporating the effects of an internal bubble. With the original TAB model, the oscillating and deforming droplet is analogous to a spring-mass system. The aerodynamic force due to the relative velocity of the droplet acts as driving force for deformation, and the surface tension force acts as restoring force. With the presence of a gas bubble inside, the aerodynamic force and the surface tension force will not change, whereas the inertial force and the viscous force will change significantly. It is assumed that the inertial force is proportional to the averaged density, and that the viscous force is proportional to the averaged viscosity coefficient. Thus, the deformation for the system can be expressed as [10]

$$\frac{\pi}{6}\left[\varepsilon\rho_{gi}+(1-\varepsilon)\rho_l\right]R_o^3\,\ddot{x}=C_F\frac{\pi}{6}\rho_{go}U^2R_o^2 - C_k\frac{\pi}{6}\sigma x - C_d\left[\varepsilon\mu_{gi}+(1-\varepsilon)\mu_l\right]\frac{\pi}{6}\dot{x}\,R_o \tag{3}$$

where x is the magnitude of deformation (distance from the equilibrium position), ε the void fraction defined as the volume ratio between the bubble and the droplet, i.e., $\varepsilon = (R_i/R_o)^3$. C_F, C_k, and C_d are model constants. With the presence of the gas bubble, these constants are expected to change slightly. However, due to lack of experimental data, they are kept the same as in the original TAB model. As in the original TAB model, breakup is assumed to occur when x reaches the droplet radius, and the secondary droplet character is determined from momentum and energy conservation.

Bubble Expansion

The exact mechanism that causes system breakup during bubble expansion is not clearly identified from the literature. It is postulated in this study that the system breakup is due to oscillations along the droplet and bubble surfaces and also that the oscillations are symmetric. The atomization occurs when the disturbance grows larger than the product of the characteristic size of the sheet and a prescribed value. The characteristic length scale for the system can be chosen as the film thickness (i.e., the difference between droplet radius R_o and bubble radius R_i), and the initial disturbance can be assumed to be proportional to the initial droplet radius R_{o0}. Therefore, the breakup criterion can be expressed as

$$K(t_b)=\frac{R_{o0}e^{\int_0^{t_b}\omega dt}}{R_o-R_i}=K_{crit} \tag{4}$$

where t_b represents the breakup time, ω is disturbance growth rate and K is the breakup variable. K_{crit} is the value of K at breakup, and it can be optimized by experimental data.

The disturbance growth rate is determined by a linear stability analysis, and its normalized form is given by [10]

$$(\Delta-\Delta^2-\Psi_o\Delta)\bar{\omega}^2+(-1+\Delta^4+\Psi_o)We_o^{1/2}\bar{\omega}+2\Delta^2 +2\Delta^{-2}-3\Psi_i\frac{We_i}{Ma_i^2}\frac{\bar{\omega}}{\bar{\omega}+3\,We_i^{1/2}}\Delta^2=0, \tag{5}$$

where

$$\bar{\omega}=\sqrt{\frac{\rho_l\overline{R_i}^3}{\sigma}}\,\omega,\quad We_o=\frac{\rho_l V_o^2\overline{R_i}}{\sigma},\quad We_i=\frac{\rho_l V_i^2\overline{R_i}}{\sigma}$$

$$Ma_i=\frac{V_i}{c},\quad \Delta=\frac{\overline{R_o}}{\overline{R_i}},\quad \Psi_o=\frac{\rho_{go}}{\rho_l},\quad \Psi_i=\frac{\rho_{gi}}{\rho_l} \tag{6}$$

Equation (6) is a cubic equation characterized by six non-dimensional variables and can be solved analytically. Three roots exist for this dispersion equation. The root with the largest real part represents the disturbance growth rate, and the imaginary part represents the frequency of oscillation.

The Sauter-mean radius (SMR) and velocity of the secondary droplets can be derived from mass, momentum and potential energy conservation before and after breakup [10].

RESULTS AND DISCUSSIONS

Aerodynamic Breakup

Using the present model for the aerodynamic breakup, the effect of bubble growth is quantified by the void fraction (i.e., the volume fraction of the internal bubble). Figure 2 gives the deformation evolution for different

void fractions. Note that the droplet radius was adjusted for each void fraction to ensure that the system has the same liquid mass. It is apparent that the deformation grows faster with increasing void fraction. Accordingly, this faster growth results in the decrease in the breakup time shown in Fig. 3.

Breakup Due to Bubble Growth

The disturbance growth rate is primarily determined by the Weber number of bubble growth We_i. Figures 4 shows the variation of disturbance growth rate versus the Weber number for a bubble-droplet system at different density ratios between bubble and liquid. As the Weber number We_i increases, the disturbance growth rate increases. In addition, the growth rate is larger for smaller density ratios between bubble and liquid.

Figure 5 shows the variation of the void fraction at breakup points ε_b versus bubble growth rate for three systems with different initial radius ratios Δ between the bubble and droplet (K_{crit} = 5 is used as the breakup criterion, although it needs to be verified by experimental data). The initial bubble diameter is 20 μm and the initial droplet diameter is 200 μm. The bubble density is 1.68 kg/m^3, the ambient gas density is 0.34 kg/m^3, and the droplet density is 626 kg/m^3. The sound speed is 220 m/s, and the surface tension coefficient is 0.00167 (Pa-m). At small growth rates V_i, the breakup void fraction ε_b is nearly independent of the bubble growth rate V_i and the initial radius ratio Δ. This suggests that for low growth rates, the atomization behavior is primarily determined by void fraction. This trend agrees with the hypothesis of Senda et al. [4] and Adachi et al. [5], which states that the breakup occurs when the void fraction is larger than a prescribed value. However, when the bubble growth rate is larger, the breakup void fraction ε_b decreases dramatically with increasing growth rate V_i, and ε_b has slightly lower values at higher radius ratios Δ.

Atomization under Flash Boiling Conditions

Five hollow-cone sprays of n-pentane from a pintle injector with different superheat degrees were simulated. The injection data were taken from Ref. 4. The parameters for each case are listed in Table 1. The computed domain is a cylindrical column with a radius of 6 cm and a height of 6 cm. For computational efficiency, a two-dimensional axisymmetric grid (120×60) was used, and 8000 parcels were used to represent the spray.

The breakup time and secondary drop size are first computed with a single parcel. The computed breakup times for the first four cases were analyzed. Computations indicate that the breakup for all cases is due to bubble expansion rather than aerodynamic force. For comparison, the breakup time of a spray computed by the Reitz and Diwakar's model [7] for the same conditions without consideration of flash boiling were obtained. For a spray with flash boiling, the breakup time decreases with decreasing ambient pressure (i.e., increasing superheat degree). For a spray without flash boiling, the breakup time increases with decreasing ambient pressure due to the decrease in air density. These results suggest that aerodynamic forces and bubble expansion compete with each other during the spray atomization process. At very low superheat degrees, the atomization can be dominated by the aerodynamical force. At high superheat degrees, the spray atomization is controlled by bubble expansion due to flash boiling. Figure 6 shows the computed SMD for the four cas-

es. A spray with higher superheat degree produces smaller SMD, and this is primarily due to an increase in bubble number density. Case 4 produces a similar SMD to Case 3, and this is because the spray atomizes at smaller void fractions for Case 4. This predicted trend for SMD is consistent with experimental observations made by Park and Lee [11]. For aerodynamic atomization, the SMD's slightly increase with increasing superheat degree due to the decrease in air density, and the SMD' s are larger than those from flash boiling.

Then spray simulation was performed for three cases. The spray parameters obtained from single parcel computations are used as the initial condition for spray simulation. Figures 7 and 8 show the position of droplets and vapor distribution for Cases 1 and 3 at a given time t = 3 ms. The spray thickness increases with increasing superheat degree. At higher superheat degrees, internal gasification occurs faster (i.e., the bubbles grow faster) resulting in faster expansion of the spray. Tip penetration slightly decreases with increasing superheat degree. This decrease is primarily due to the smaller drop sizes, which result in faster vaporization and more momentum transfer from the droplet to the gas. The effect of smaller drop sizes is somehow cancelled by the effect of lower ambient pressure that tends to increase tip penetration. In addition, fuel vapor penetrates further in the radial direction for higher superheat degrees.

In the first four cases listed in Table 1, different superheat degrees were produced by varying the ambient pressure. It would be interesting to vary the fuel and ambient temperature as well since VanDerWege and Hochgreb [12] observed that the spray shows a completely different structure at a high engine head temperature. Therefore, a simulation was made for Case 5, which has the same ambient pressure as Case 1, but has a higher fuel and ambient temperature of 353 K. A plot of droplet positions and vapor distribution is shown in Fig. 9. A spray pattern completely different from that of Case 1 was obtained, and the spray shifts to a near solid-cone structure, as observed in the experiment [8]. Computational results support the explanation of VanDerWege and Hochgreb [12] that this shift is due to flash boiling and air-entrainment. The entrained air brings the smaller droplets produced from flash boiling into the core of the hollow cone, and this results in the inward collapse of the hollow cone.

CONCLUSIONS

A model for atomization with intermediate superheat degrees has been developed and was applied to predict the atomization of hollow-cone sprays under flash boiling conditions. The results can be summarized as follows.

(1) For disturbances due to aerodynamic force, the presence of a bubble results in an increase in the disturbance growth rate and a decrease in breakup time and secondary drop size.

(2) For bubble expansion, the disturbance growth rate of the bubble-droplet system is primarily dependent on the Weber number of bubble growth rate.

(3) Aerodynamic forces and bubble expansion compete with each other during the atomization under flash boiling conditions. Aerodynamic forces dominate the regime of low superheat degree, while bubble expansion dominates the regime of high superheat degree. In the regimes this study considered (4 K < ΔT < 64 K), sprays are atomized by bub-

ble expansion, which produces smaller SMD' s than aerodynamic forces alone.

Acknowledgement

This work was supported in part by the National Science Foundation under grant No. CTS-9734402, with Farley Fisher as technical monitor, and by Ford Motor Company.

REFERENCES

1. Kim, Y. K., Twai, N., Suto, H., and Tsuruga, T., "Effect of Air Motion on Fuel Spray Characteristics in a Gasoline Direction Injection Engine", *JSAE Review*, Vol. 1, pp. 81 -86 (1980).
2. Lienhard, H., and Day, J. B., "Temperature and Scale Effects Upon Cavitation and Flashing in Free and Submerged Jets" *Journal of basic Engineering*, Vol. 88, pp. 515-522 (1970).
3. Oza, R. D., and Sinnamon, J. F., "An Experimental and Analytical Study of Flash-Boiling Fuel Injection", SAE Paper 830590 (1983).
4. Senda, J., Yamaguchi, M., Tsukamoto, T. and Fujimoto, H., "Characteristics of Spray Injected from Gasoline Injector", *JSME International Journal Series B*, Vol. 37, pp. 931-936 (1994).
5. Adachi, M., McDonell, V. G., Tanaka, D., Senda, J. and Fujimoto, H., "Characterization of Fuel Vapor Concentration inside a Flash Boiling Spray", SAE Paper 970871 (1997).
6. Razzaghi, M., "Droplet Size Estimation of Two-Phase Flashing Jets", *Nuclear Engineering and Design*, Vol. 114, pp. 115-124 (1989).
7. Reitz, R. D., and Diwakar, R., "Structure of High-Pressure Fuel Sprays", SAE Paper 870598 (1987).
8. Plesset, M. S., and Zwick, S. A., "The Growth of Vapor Bubbles in Superheated Liquids", *Journal of Applied Physics*, Vol. 25, No. 4, pp. 492-500 (1954)
9. O' Rourke, P. J. and Amsden, A. A., "The TAB Method for Numerical Calculation of Spray Droplet Breakup", SAE Paper 872089, (1987).
10. Zeng, Y., "Modeling of Multicomponent Fuel Vaporization in Internal Combustion Engines", Ph. D. Thesis, University of Illinois at Urbana-Champaign, (2000).
11. Park, S. and Lee, S. Y. "An Experimental Investigation of the Flash Atomization Mechanism, *Atomization and Sprays*", Vol. 4, pp. 159-179 (1994).
12. Vanderwege, B. and Hochgerb, S., "The Effect of Fuel Volatility on Spays from High Pressure Swirl Injectors", *26th Symposium on Combustion*, pp. 1865-1871 (1998).

Table 1 Parameters for Five Cases

	Pamb	Liquid temperature	ΔT
Case 1	48 kPa	293 K	4.2 K
Case 2	35 kPa	293 K	11.9 K
Case 3	21 kPa	293 K	23.5 K
Case 4	14 kPa	293 K	31.9 K
Case 5	48 kPa	353 K	64.2 K

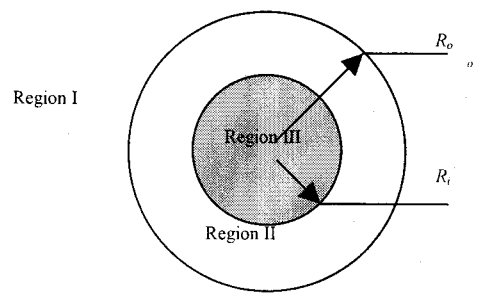

Fig. 1 Schematic of bubble/droplet

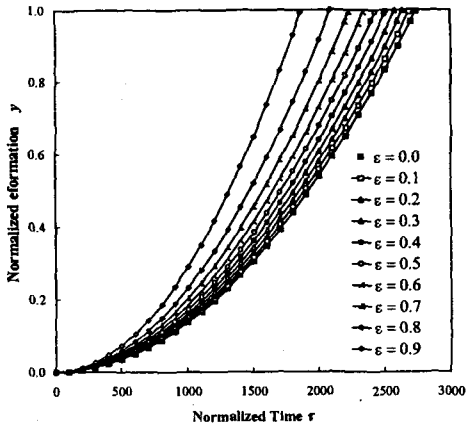

Fig. 2 Variation of deformation versus normalized time

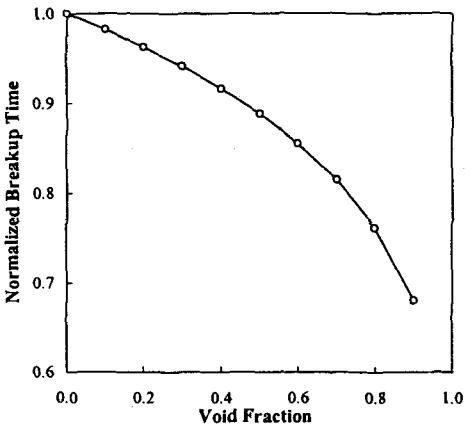

Fig. 3 Variation of breakup time versus void fraction

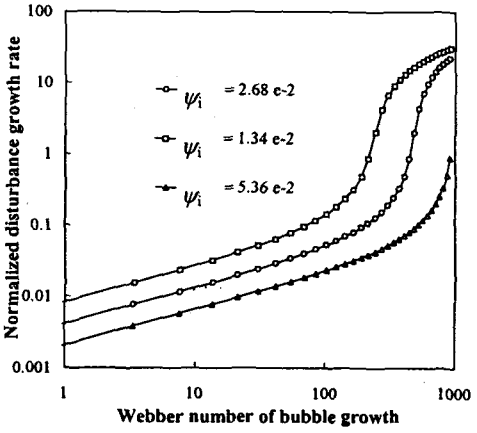

Fig. 4 Variation of disturbance growth rate versus Weber number at different density ratios between bubble and liquid

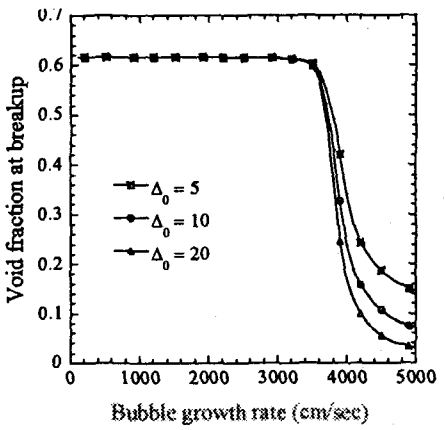

Fig. 5 Void fraction at system breakup system versus bubble growth rate

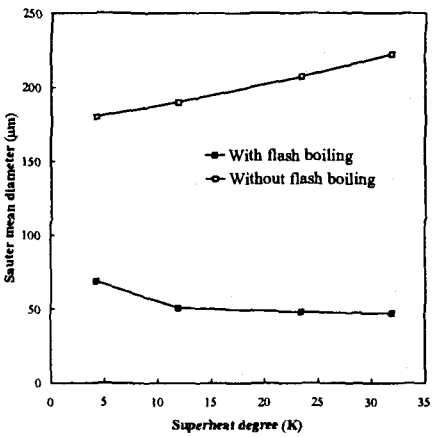

Fig. 6 The variation of SMD versus superheat degree

Fig. 7 Plots of droplet position and vapor distribution for Case 1

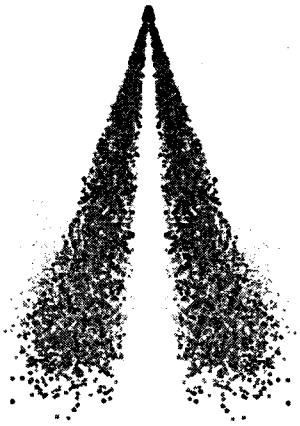

Fig. 8 Plots of droplet position and vapor distribution for Case 3

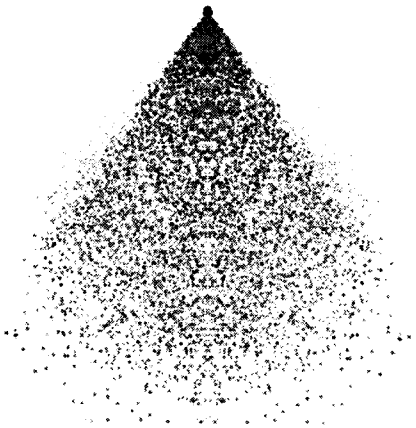

Fig. 9 Plots of droplet position and vapor distribution for Case 5